



Methyl orange removal from aqueous solutions by natural and treated skin almonds

F. Atmani^{a,b,*}, A. Bensmaili^b, A. Amrane^{c,d}

^aFaculté des sciences de l'ingénieur, Université Saad Dahlab Blida, Algérie
email: datmani@yahoo.fr

^bLaboratoire de génie de la réaction, Faculté de génie mécanique et génie des procédés, Université des sciences et de la technologie Houari Boumediene, BP 32El Alia Bab Ezzouar, Alger, Algérie

^cEcole Nationale Supérieure de Chimie de Rennes, CNRS, UMR 6226, Avenue de Général Leclerc, CS 50837, 35708 Rennes Cedex, France

^dUniversité européenne de Bretagne

Received 7 December 2009; Accepted 26 April 2010

ABSTRACT

The aim of this study was to explore the feasibility of using skin almonds (SA), a new agricultural sorbent, for the removal of hazardous dye methyl orange (MO). The first objective of this work was to examine the influence of different chemical treatments on the adsorption capacity of SA. The treatment of SA with alkaline solution as well as with salt solution decreased the sorption ability for MO, whereas the acidic treatment increased markedly the sorption ability for the anionic dye. The next objective was to evaluate the properties of the adsorbent, the effect of the contact time, the temperature, the dye concentration and the particles size. Adsorption of the dye on both adsorbents (natural and treated) has been monitored through the Langmuir, Freundlich and Redlich-Peterson adsorption isotherm models and it was shown that the adsorption process followed as Freundlich isotherm, which led to the higher correlation coefficient. Two kinetic models, pseudo second order and Elovich equation were employed to analyze kinetics data. It was found that the pseudo second-order was the most relevant to describe the adsorption behavior. In addition, the activation energy was also determined based on the pseudo-second order rate constants.

Keywords: Adsorption; Dye; Kinetic; Methyl orange; Skin almonds

1. Introduction

Dyes are extensively used in paper, textile, dye houses and printing to color the final products [1]. They usually have a synthetic origin and complex aromatic structures making them more stable to be degraded [2] and are classified as anionic, cationic and nonionic dyes [3]. Existing colored wastewater treatment methods involve in a combination of physical and chemical processes. Various treatment methods such as coagulation, precipitation, ultrafiltration,

ozonation, oxidation and reverse osmosis have been applied in removing dyes from wastewaters. However, adsorption is considered superior compared with other traditional treatment methods due to its easy availability, simplicity of design, high efficiency, ease of operation and ability to remove colored contaminants from wastewaters. Recently, attentions have been focused on the development of low cost adsorbent for the application concerning treatment of wastewater [4,5]. Skin almonds (SA), being a low cost and easily available adsorbent, could be an alternative for more costly wastewater treatment processes [6]. To the best of our knowledge, there is no information in

*Corresponding author.

literature on the use of SA as an adsorbent. In this work, the potentials for the use of SA, a new agricultural sorbent, as an adsorbent for methyl orange (MO) removal from solutions was investigated.

2. Materials and methods

2.1. Adsorbate

The acid dye MO is widely used in the textile, pharmaceutical and paper manufacturing. Double distilled water was employed for preparing all the solutions.

2.2. Preparation, characterisation and pre-treatment of adsorbent

SA were obtained locally. The precursor was first washed with distilled water for several times and dried in an oven at 100 °C for 2 h, grounded and sieved to get particle of uniform geometrical dimensions (0.50–0.85 mm).

The surface area of the SA was measured by BET (Brunauer-Emmett-Teller nitrogen adsorption technique). The point of zero charge of the sample is determined by the solid addition method [7]. The physical characteristics of this adsorbent are listed in Table 1.

Studies were carried out using two different SA forms, natural and treated, the adsorbent material designed as natural skin almonds (NSA) and its treated form treated skin almonds (TSA). SA were treated by three different types of chemical treatments: acidic (H_2SO_4), alkaline (NaOH) and salt treatment ($MgCl_2$). Sample of 100 g of SA was mixed with solution of the considered reagent. The mixture was stirred for different times (Table 2). The sample was then washed several times with distilled water and filtered, the optimization of chemical treatment operating conditions was then carried out based on a plan experiments involving three parameters, the temperature, the contact time and the chemical concentration of the solution reagent (H_2SO_4 , NaOH and $MgCl_2$), which were considered at two levels, 50 and 70 °C for the temperature, 2 and 4 h for the contact time, and 1 and 2 mol/l for the concentration reagent. The plan consisted therefore in 8 experiments for each chemical reagent (Table 2).

Table 1
Physical characteristics of SA and H_2SO_4 treated SA

| Parameters | NSA | TSA |
|--|-------|-------|
| Humidity | 5.4 | 6.5 |
| Apparent density (g/cm ³) | 0.254 | 0.199 |
| True density(g/cm ³) | 0.420 | 0.355 |
| Porosity (%) | 65.0 | 69.5 |
| Total void volume (cm ³ /g) | 1.556 | 2.208 |
| Surface area (m ² /g) | 4.0 | 5.5 |
| pH _{PZC} | 10.03 | 9.97 |

Table 2

Plan experiments for the optimization of the operating conditions of SA treatment

| Chemical reagent (H_2SO_4 , NaOH or $MgCl_2$) | | | |
|---|------------------|-----------------------|--------------------|
| Experiment | Temperature (°C) | Concentration (mol/l) | Treatment time (h) |
| 1 | 70 | 2 | 4 |
| 2 | 70 | 2 | 2 |
| 3 | 50 | 2 | 4 |
| 4 | 50 | 2 | 2 |
| 5 | 70 | 1 | 4 |
| 6 | 70 | 1 | 2 |
| 7 | 50 | 1 | 4 |
| 8 | 50 | 1 | 2 |

2.3. Adsorption kinetic study

The adsorbent mass (0.3 g) was mixed with 50 ml of the desired dye concentration at the required temperature in conical flasks. Sorption experiments were carried out in batch; the initial sorbent concentration and the solution temperature were examined. Samples were withdrawn at suitable time intervals and were separated from the sorbent by centrifugation for 20 min. The amount of dye adsorbed on natural and modified SA was calculated indirectly from the difference of dye concentration in solution before and after sorption experiment. The dye concentration was determined by measuring the absorbance of the solution using UV-visible spectrophotometer at a maximum wavelength of 466 nm. Experiments were repeated at initial MO solution pH of 4 for various initial dye concentrations (5, 20, 30 and 40 mg/l); temperature (23, 30, 40 and 50 °C) values and particles size (500, 750 and 850 μm).

2.4. Equilibrium studies

Adsorption experiments were carried out by adding a fixed amount of adsorbent (0.3 g) to a series of conical flasks filled with 50 ml diluted dye solutions. The conical flasks were placed in a thermostatic shaker at 23, 30, 40 and 50 °C. The experiments were carried out at initial solution pH of 4 and particle size values ranging from 500 to 850 μm. Removal efficiency (E) of dye on SA and, sorption capacity, (q), were calculated from Eqs. (1) and (2):

$$E(\%) = \frac{C_i - C_f}{C_i} 100 \quad (1)$$

$$q = \frac{V(C_i - C_f)}{m} \quad (2)$$

where C_i and C_f were the initial and final dye concentrations (mg/l) in aqueous solutions, respectively, V was

the volume of the solution (l) and m represented the weight of adsorbent (g).

3. Results and discussion

3.1. Effect of the chemical treatment on the adsorption of MO

Fig. 1 shows the results for the removal of MO by natural and treated SA. Among the different chemical treatment used, treatment with H_2SO_4 appeared to be the most effective for SA. Indeed, during this activation process, considerable amount of cations were most likely substituted by hydrogen cations which increases the specific active area. Furthermore, acids are polar molecules which improve their diffusion. It was observed that the percentage removal of MO increases from 37.5% without treatment to 78.1% when treated by H_2SO_4 (2 mol/l, $T = 70^\circ C$ and 4 h treatment time). The adsorption capacity of the tested SA also increased after NaOH or $MgCl_2$ treatment but to a lower extent, 45 and 52% at best with

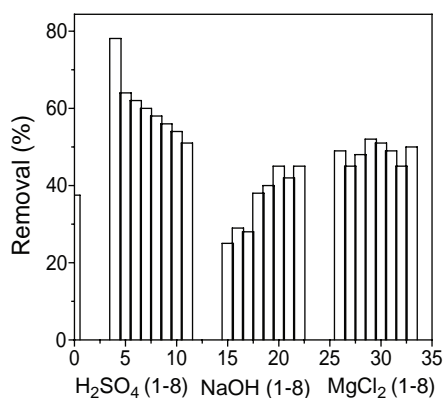


Fig. 1. Effect of the chemical treatment on the adsorption of MO.

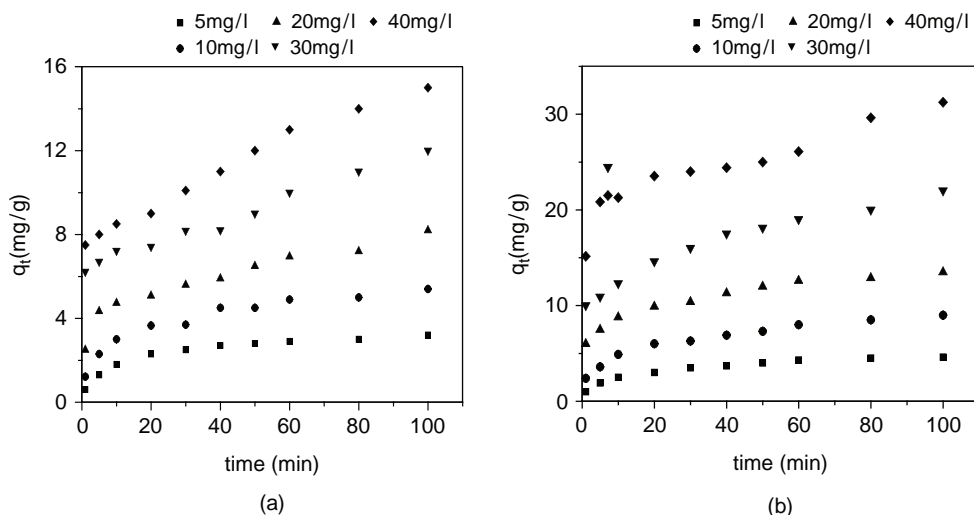


Fig. 2. Time-courses of the adsorption capacity of (a) non-treated; and (b) treated SA for various initial MO concentrations.

NaOH. It should be noted that on one hand NaOH treatment appeared somewhat too aggressive since in almost all cases 2 mol/l led to a lower adsorption capacity than the non-treated SA, and on the other hand the efficiency of the $MgCl_2$ treatment remained nearly the same irrespective of the operating conditions. Consequently MO removal studies were carried out using different SA forms, natural and treated in the optimal conditions, namely 2 mol/l H_2SO_4 , $70^\circ C$ and 4 h contact time.

3.2. Time dependent adsorption

Contact time is one of the important parameters for successful deployment of the adsorbent for practical application and rapid adsorption is among desirable parameters [8]. A rapid uptake of pollutants and establishment of equilibrium in a short period signifies the efficacy of that adsorbent for its use in wastewater treatment. The effect of contact time for the adsorption of MO by natural and treated SA was studied for a period of 100 min for various initial concentrations and different temperatures.

3.2.1. Effect of contact time on adsorption at different concentrations

The effect of initial dye concentration and contact time on MO adsorption is shown in Fig. 2. Fig. 2 indicates that the sorption increased for increasing contact time and become almost constant at 100 min. Generally, when adsorption involves a surface reaction process, the initial adsorption is rapid.

The effect of the initial MO concentration on adsorption by SA was investigated in the range of 5–40 mg/l initial dye concentration. As observed, the higher the initial concentration of dye, the larger was the amount of dye

adsorbed, which was consistent with studies previously reported [9]. The increase in uptake capacity of the sorbent with increasing dye concentration may be due to the increase of sorbate quantity. The amount of MO adsorbed increased from 3.2 to 15 mg/g and from 4.6 to 31.3 mg/g as the initial adsorbate concentration increased from 5 to 40 mg/l for natural and treated SA respectively. However, for the same adsorbent (treated or non-treated SA) and contact time, there is a drop in the relative removal efficiency for increasing dye concentration, most likely due to a saturation of the adsorption sites.

3.2.2. Effect of contact time on adsorption at different temperatures

Fig. 3 indicates the MO dye uptake by the natural and treated SA as a function of contact time at different

temperatures of 23, 30, 40 and 50 °C. As can see from this figure, an uptake capacity of 6 mg/g was observed within 1 min and then the adsorption capacity was increased constantly with increasing contact time reaching to a maximum point of 13.5 mg/g in 100 min at 23 °C. A similar trend was observed at 30, 40 and 50 °C. Therefore, 100 min is enough to achieve the adsorption equilibrium.

3.3. Effect of the particle size

The influence of the adsorbent particle size was investigated at constant pH 4, 20 mg/l of dye, 500 rpm agitation speed and 23 °C by using three selected particles sizes (500, 750 and 850 μm) of SA (Fig.4). The amount of dye adsorbed increased from 10.9 to 13.5 mg/g for a decrease in the adsorbent particle size from 850 to 500 μm. Variation of the adsorption conversely to the

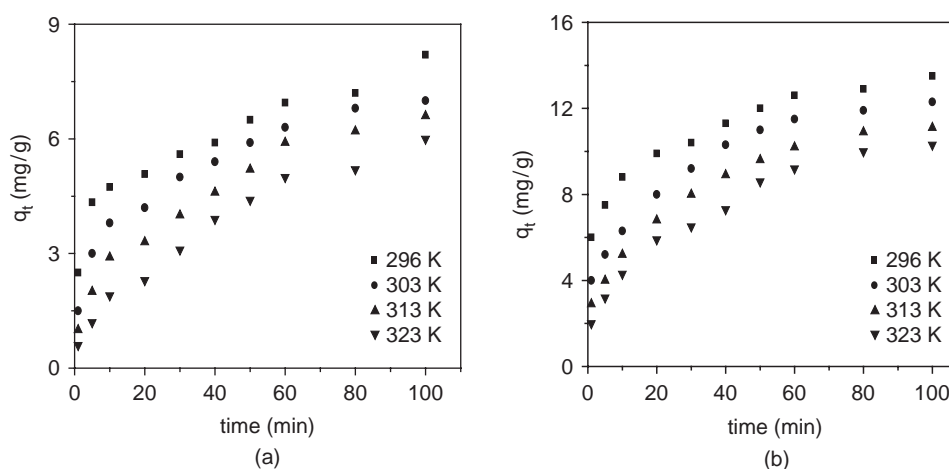


Fig. 3. Effect of contact time on adsorption of MO by the (a) natural; and (b) treated SA at various temperatures.

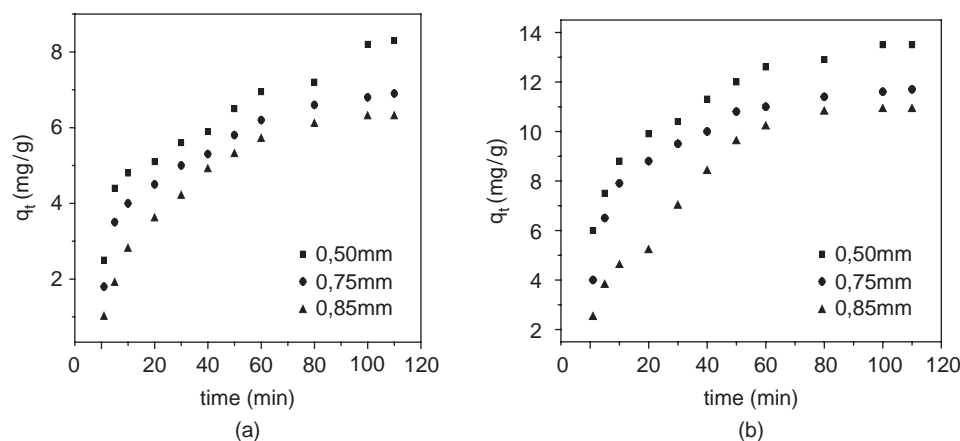


Fig. 4. Effect of the particle size on (a) natural; and (b) treated SA on dye adsorption.

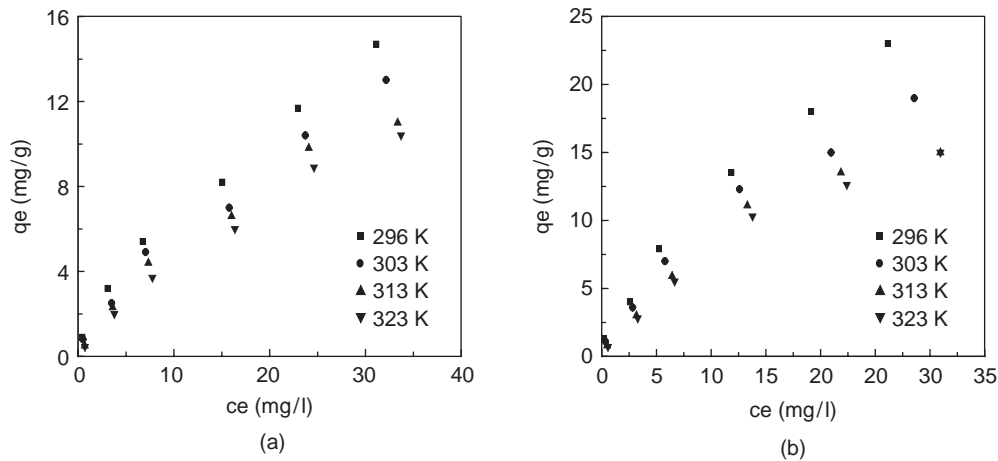


Fig. 5. Dye adsorption of MO of (a) natural; and (b) treated SA at various temperatures.

particle size should be related to the increase of the effective specific surface area when particle size was lowered. Higher dye adsorption of small particles can also be related to improving mass transport inside the sorbent particle; in agreement with previous report [10].

3.4. Equilibrium modelling

When the system is in the state of equilibrium distribution of dye between the adsorbent and the dye solution is important to establish the capacity of the adsorbent for the dye. Fig. 5 shows the experimental curves of q_e vs c_e for the adsorption of MO at four constant temperatures of 23, 30, 40 and 50 °C. It was found that dye uptake capacity q_e of SA increased for decreasing temperatures indicating the exothermic nature of the adsorption reaction. For increasing temperature from 23 to 50 °C, the MO removal decreased from 23 to 15 mg/g; similar result was also observed for MO removal from wastewaters using De-oiled Soya and Bottom Ash [11].

The isotherm data were treated using three of the most commonly used equilibrium models, Langmuir, Freundlich and Redlich-Peterson equilibrium isotherm theories. The forms of these isotherms are presented by the following equations:
Langmuir model [12]

$$q_e = q_{\max} \frac{bC_e}{1 + bC_e} \quad (3)$$

In Eq. (3), q_e is the adsorption capacity at equilibrium. C_e is the equilibrium concentration, and q_{\max} and b are the Langmuir constants related to the maximum adsorption capacity and the adsorption energy respectively. Four different types of linearization can be used for the Langmuir isotherm, the widely used linear expression is

$$\frac{C_e}{q_e} = \frac{1}{q_{\max}b} + \frac{C_e}{q_{\max}} \quad (4)$$

q_{\max} and b can be determined from the linear plot of C_e/q_e versus C_e .

The Freundlich model [13]

The empirical model was shown to be consistent with an exponential distribution of active centers, characteristics of heterogeneous surfaces. The amount of solute adsorbed, q_e is related to the concentration of solute in the solution, c_e , as following:

$$q_e = K_f C_e^{1/n} \quad (5)$$

where q_e is the adsorption capacity at equilibrium. C_e is the equilibrium concentration K_f and n are the Freundlich constants, n giving an indication of how favourability of the adsorption process and K_f is the adsorption capacity of the adsorbent. A linear form of the Freundlich expression can be obtained by taking logarithms of Eq. (5)

$$\ln q_e = \ln K_f + \frac{1}{n} C_e \quad (6)$$

The Redlich-Peterson model [14]

$$q_e = \frac{AC_e}{1 + BC_e^\beta} \quad (7)$$

The Redlich-Peterson equation involves three parameters A , B and β ($0 < \beta < 1$). A and B are constants, and β is the degree of heterogeneity. This model is used to describe chemical and physical adsorption on heterogeneous surface.

When $\beta = 1$, It becomes a Langmuir equation

$$q_e = \frac{AC_e}{1 + BC_e} \tag{8}$$

And for $\beta = 0$, it leads to the Henry's law:

$$q_e = \frac{AC_e}{1 + B} \tag{9}$$

Eq. (7) can be converted to a linear form by taking logarithms:

$$\ln\left(A \frac{C_e}{q_e} - 1\right) = \ln B + \beta \ln C_e \tag{10}$$

To deduce the isotherm constants from the linear form of Redlich-Peterson equation, the value of the parameter A has to be estimated based on linear regression.

The model parameter values estimated from Eqs. (4), (6) and (10) by linear regression analyses, as well as the correlation coefficients (R^2) are collected in Table 3.

A comparison of the experimental isotherms with the adsorption isotherm models showed that the Freundlich model yielded the best fit for both MO-NSA and MO-TSA systems, with R^2 values equal or higher than 0.984 if compared to the others two models. Conformation of the experimental data into Freundlich isotherm equation indicated the heterogeneous nature of SA surface. In all cases the Freundlich and Redlich-Peterson equations represents a better fit of experimental data than Langmuir equation. However, in comparison between R^2 values for Freundlich and Redlich-Peterson isotherm fit, Freundlich isotherm shows better fit.

The n parameter of the Freundlich equation ($1.22 < n < 1.65$) revealed adsorption sites with low energetic heterogeneity of this natural adsorbent [15]. Both K_f

Table 3

Langmuir, Freundlich and Redlich-Peterson isotherm model constants and correlation coefficients for adsorption of MO on natural and treated SA

| Systems | Isotherms | Solution temperature (°C) | Constants | | | |
|---------|------------------|---------------------------|-----------|------|---------|-------|
| | | | q_{max} | b | R^2 | |
| MO-NSA | Langmuir | 23 | 20.2 | 0.06 | 0.880 | |
| | | 30 | 19.2 | 0.05 | 0.832 | |
| | | 40 | 20.2 | 0.03 | 0.961 | |
| | | 50 | 21.1 | 0.03 | 0.951 | |
| MO-TSA | Langmuir | 23 | 31.9 | 0.07 | 0.815 | |
| | | 30 | 26.7 | 0.07 | 0.894 | |
| | | 40 | 24.6 | 0.05 | 0.945 | |
| | | 50 | 27.1 | 0.04 | 0.956 | |
| MO-NSA | Freundlich | | K_f | n | R^2 | |
| | | 23 | 1.51 | 1.54 | 0.999 | |
| | | 30 | 1.20 | 1.48 | 0.996 | |
| | | 40 | 0.75 | 1.25 | 0.994 | |
| MO-TSA | Freundlich | 23 | 2.92 | 1.65 | 0.984 | |
| | | 30 | 2.12 | 1.53 | 0.993 | |
| | | 40 | 1.30 | 1.33 | 0.990 | |
| | | 50 | 1.13 | 1.27 | 0.993 | |
| MO-NSA | Redlich-Peterson | | A | B | β | R^2 |
| | | 23 | 6.2 | 0.66 | 0.63 | 0.989 |
| | | 30 | 11.2 | 0.70 | 0.55 | 0.992 |
| | | 40 | 12.5 | 1.12 | 0.25 | 0.994 |
| MO-TSA | Redlich-Peterson | 23 | 8.5 | 0.79 | 0.65 | 0.956 |
| | | 30 | 7.8 | 0.72 | 0.45 | 0.991 |
| | | 40 | 8.0 | 0.46 | 0.33 | 0.985 |
| | | 50 | 6.0 | 0.89 | 0.15 | 0.990 |

and n parameter values were achieved at 23°C, showing that binding capacity reached its highest value and that the affinity between the sorbent and dye ions was also higher than for the other temperature investigated (Table 3).

3.5. Kinetic models

Adsorption equilibrium study is important to determine the effectiveness of adsorption. Two different models to predict the adsorption kinetic of MO on SA were considered, the pseudo-second order and the Elovich models.

Based on equilibrium adsorption, the pseudo-second order kinetic Eq. [16] is expressed as:

$$\frac{t}{q_t} = \frac{1}{K_2 q_e^2} + \frac{1}{q_e} t \quad (11)$$

where k_2 is the equilibrium rate constant of pseudo-second order adsorption (g/mg min).

The simple Elovich model has been also successfully used to describe second order kinetic assuming that the actual solid surfaces are energetically heterogeneous [17]; the linear form of this equation is given by:

$$q_t = a + b \ln t \quad (12)$$

The Elovich coefficients could be computed from the plots q_t versus $\ln t$, the initial adsorption rate a and the desorption constant b were calculated from the intercept and the slope of the straight line of q_t against $\ln t$.

The kinetic constants of both models are collected in Table 4. The kinetic constants obtained from the Elovich equation varied as a function of the initial MO concentration and solution temperature.

Based on the R^2 values and a comparison between the experimental and calculated q_e values, it can be seen that the kinetic of MO adsorption onto SA followed a pseudo-second model with correlation coefficient higher than 0.928, the equilibrium adsorption capacity, q_e , increased as the initial dye concentration, C_i , increased from 5 to 40 mg/l. It was also found that the variations of the rate constant, K_2 , seemed to have a decreasing trend with increasing initial dye concentration. Similar phenomena have been previously reported in the adsorption of methylene blue by hazelnut shells and wood sawdust [18], acid blue 193 onto BTMA-bentonite [19] and adsorption of basic black dye using calcium alginate beads [20]. The variations of t/q_t versus t at various temperatures of dye solutions for an initial concentration of 20 mg/l still confirmed the adequation of the pseudo-second-order model to fit experimental data. The results in Table 4 reported that

Table 4
Parameters for pseudo-second order and Elovich models

| C_i (mg/l) | T (°C) | $q_{e,exp}$ (mg/g) | Pseudo-second order model | | | Elovich model | | | |
|--------------|----------|--------------------|---------------------------|------------------|-------|--------------------|-------|------|-------|
| | | | $q_{e,cal}$ (mg/g) | K_2 (g/mg min) | R^2 | $q_{e,cal}$ (mg/g) | a | b | R^2 |
| MO-NSA | | | | | | | | | |
| 5 | 23 | 3.2 | 3.4 | 0.035 | 0.996 | 3.2 | 0.51 | 0.58 | 0.996 |
| 10 | 23 | 5.4 | 5.6 | 0.019 | 0.988 | 5.2 | 0.98 | 0.91 | 0.989 |
| 20 | 23 | 8.2 | 8.2 | 0.013 | 0.979 | 7.3 | 2.30 | 1.08 | 0.974 |
| 30 | 23 | 12.0 | 12.0 | 0.009 | 0.963 | 10.3 | 5.07 | 1.14 | 0.858 |
| 40 | 23 | 15.0 | 16.5 | 0.005 | 0.946 | 13.2 | 5.79 | 1.62 | 0.884 |
| 20 | 23 | 8.2 | 8.2 | 0.013 | 0.979 | 7.3 | 2.30 | 1.08 | 0.974 |
| 20 | 30 | 7.0 | 7.5 | 0.012 | 0.985 | 6.7 | 1.12 | 1.21 | 0.985 |
| 20 | 40 | 6.6 | 7.4 | 0.008 | 0.964 | 6.0 | 0.28 | 1.25 | 0.962 |
| 20 | 50 | 6.0 | 7.2 | 0.005 | 0.928 | 5.2 | -0.34 | 1.19 | 0.938 |
| MO-TSA | | | | | | | | | |
| 5 | 23 | 4.6 | 4.9 | 0.021 | 0.991 | 4.5 | 0.74 | 0.82 | 0.991 |
| 10 | 23 | 9.0 | 9.4 | 0.010 | 0.985 | 8.5 | 1.76 | 1.46 | 0.982 |
| 20 | 23 | 13.5 | 13.9 | 0.012 | 0.993 | 13.6 | 4.87 | 1.89 | 0.937 |
| 30 | 23 | 22.0 | 22.3 | 0.005 | 0.985 | 20.0 | 7.81 | 2.65 | 0.946 |
| 40 | 23 | 31.2 | 31.0 | 0.005 | 0.981 | 28.7 | 14.78 | 3.01 | 0.950 |
| 20 | 23 | 13.5 | 13.9 | 0.012 | 0.993 | 13.6 | 4.87 | 1.89 | 0.937 |
| 20 | 30 | 12.3 | 13.2 | 0.008 | 0.990 | 12.0 | 2.75 | 2.00 | 0.969 |
| 20 | 40 | 11.1 | 12.2 | 0.007 | 0.987 | 10.7 | 1.63 | 1.97 | 0.969 |
| 20 | 50 | 10.3 | 11.5 | 0.005 | 0.972 | 9.65 | 0.73 | 1.94 | 0.962 |

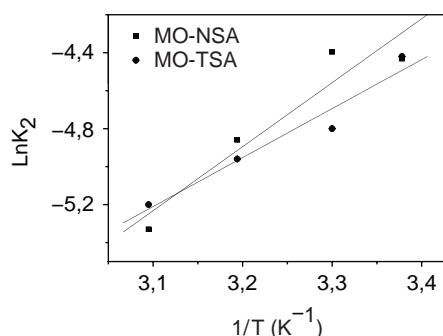


Fig. 6. Arrhenius plots for adsorption of MO onto SA at various temperatures.

the rate constant, K_2 , of the pseudo-second-order model for MO adsorption onto treated SA decreased from 0.012 to 0.005 g/mg min with increase in the solution temperature from 23 to 50 °C. It is probably due to change of mechanism of MO adsorption onto SA upon changing the temperature. Similar behavior was obtained for the adsorption of basic dye [21], acid dye [11] and heavy metal [22].

These results imply that the adsorption system studied follows to the pseudo second order kinetic model at all variables.

The second-order rate constant can be expressed as a function of the temperature by the Arrhenius Eq. [23]. K_0 is the temperature independent factor (g/mg min) and E_a is the activation energy of sorption (kJ/mol).

$$K_2 = K_0 e^{\frac{-E_a}{RT}} \quad (13)$$

To calculate activation energy (E_a) for adsorption process, $\ln K_2$ is plotted versus $1/T$ (Fig. 6). The magnitude of activation energy gives an idea about the type of adsorption which is mainly physical or chemical. The physisorption processes usually have energies in the range of 5–40 kJ/mol while higher activation energies (40–800 kJ/mol) suggest chemisorptions [24–26].

The activation energy values were found to be –28.19 and –20.95 KJ/mol for MO-NSA and MO-TSA respectively; showing that dye adsorption onto natural or treated SA was an exothermic process. Moreover, these low activation energy values confirmed that the adsorption process was governed by physisorption.

4. Conclusion

SA, an agricultural waste, were successfully employed with H_2SO_4 treatment to remove acid dye. The results showed that the adsorption was dependent on the initial dye concentration and the temperature solution. Adsorption equilibrium for both systems, untreated and treated SA, followed a Freundlich isotherm. Two kinetic models, pseudo-second order and Elovich models were tested to investigate the adsorption mechanism. Irrespective of the initial dye concentration and the running temperature, both models matched experimental data, even if the pseudo-second order kinetic model led to the best fit.

References

- [1] Z. Aksu, A review Process Biochem., 40 (2005) 997–1026.
- [2] Z. Aksu, S. Tezer, Process Biochem., 40 (2005) 1347–1361.
- [3] Y. Fu, T. Viraraghavan, A review, Bioresour. Technol., 79 (2001) 251–262.
- [4] C. Namasivayam, M.D. Kumar, K. Selvi, R.A. Begum, T. Vanathi, R.T. Yamuna, Biomass Bioenergy, 21 (2001) 477–483.
- [5] E. Forgacs, T. Cserhati, G. Oros, A review, Environ. International, 30 (2004) 953–971.
- [6] F. Atmani, A. Bensmaili, N.Y. Mezener, Environ. Sci. Technol., 2 (2009) 153–169.
- [7] S.K. Mishra and S.B. Kanungo, R. Rajeev, J Colloid. Interface Sci., 267 (2003) 4248.
- [8] T. Akar and S. Tunali, Miner. Eng., 18 (2005) 1099–1109.
- [9] N. Yeddou and A. Bensmaili, Chem. Eng. J., 119 (2006) 121–125.
- [10] I.D. xMall, V.C. Srivastava, N.K. Dyes and Pigments, 69 (2006) 210–223.
- [11] A. Mittal, A. Malviya, D. Kayr, J. Mittal, L. Kurup, J. Hazard. Mater., 148 (2007) 229–240.
- [12] J.X. Lin, S.L. Zhan, M.H. Fang, X.Q. Qian, H. Yang, J. Environ. Manag., 87 (2008) 193–200.
- [13] I.A.W. Tan, A.L. Ahmad, B.H. Hameed, Colloids and Surf., 318 (2008) 88–96.
- [14] Y. Xue, H. Hou, S. Zhu, Chem. Eng. J., 147 (2009) 272–279.
- [15] M.M. Dávila-Jimenez, M.P. Elizalde-Gonzalez, A.A. Peláez-Cid, J Colloid Interface Sci., A254 (1–3) (2005) 107–114.
- [16] Y.S. Ho, J. Hazard. Mater. B136 (2006) 681–689.
- [17] D.L. Sparks, Kinetics of soil chemical processes, New York, Academic Press In 1989.
- [18] F. Ferrero, Dye, J. Hazard. Mater., 142 (2007) 144–152.
- [19] A.s. Ozcan, B. Erdem, A. Ozcan, Colloids Surf. A., 266 (2005) 73–81.
- [20] R Aravindhan, N.F. Nishad, Colloids Surf. A., 299 (2007) 232–238.
- [21] M. Al-Ghouti, M.A.M. Khraisheh, M.N.M. Ahmad, S. Allen, J Colloid Interface Sci., 287 (2005) 6–13.
- [22] S. Erenturk, E. Malkok., Appl. Surf. Sci., 253 (2007) 4727–4733.
- [23] C. Namasivayam and R.T. Yamuna, Chemosphere, 30 (3) (1995) 561–578.
- [24] H. Nollet, M. Roels, P. Lutgen, P. Van Der Meeren, W. Verstraete, Chemosphere, 53 (2003) 655–665.
- [25] M. Dogan, H. Abak, M. Alkan, J. Hazard. Mater., 164 (2009) 172–181.
- [26] B.H. Hameed, A.A. Ahmad, N. Aziz, Chem. Eng. J., 133 (2007) 195–203.